Application of TWDEC Simulator to End-loss Flux of GAMMA 10 Tandem Mirror

Hiromasa TAKENO, Long C. BAI, Masahiro KUME, Yasuyoshi YASAKA, Yousuke NAKASHIMA[1)]

Department of Electrical and Electronic Engineering, Kobe University, Kobe 657-8501, Japan
[1)] *Plasma Research Center, University of Tsukuba, Tsukuba 305-8577, Japan*

(Received: 30 October 2009 / Accepted: 5 February 2010)

The operation characteristics of traveling wave direct energy converter (TWDEC), which was expected to be used for direct energy conversion of fast protons produced in an advanced fusion, was studied in the condition that the incident particle flux had a wide energy spread. The end-loss flux of GAMMA 10 tandem mirror was employed as the incident flux, as it had a broad energy spectrum. The bias-type TWDEC was constructed and installed at the end of GAMMA 10, and the initial experimental result was presented. The result was not inconsistent with an expected TWDEC characteristics. For the next full-scale experiment, the design of modulator and decelerator was examined. The more efficient design was presented for the incident flux with a broad energy spectrum.

Keywords: advanced fusion, direct energy conversion, TWDEC, GAMMA 10, wide energy spread, bias-type TWDEC

1. Introduction

Traveling wave direct energy converter (TWDEC) was proposed as a device for direct energy conversion from high energy protons produced in D-^{3}He fusion reaction[1]. Huge part of the output energy of D-^{3}He fusion reactor is carried by kinetic energy of protons, the energy of which is too enormous to convert by a conventional electrostatic energy converter. Thus, the development of TWDEC is one of the most important issues to realize an efficient fusion power plant acceptable in a sustainable society.

The TWDEC consists of a modulator and a decelerator. Fast protons from the reactor are guided into the modulator where radio frequency (RF) electric field modulates their velocity. The modulated proton beam is bunched in the downstream where the decelerator exists. This density-modulated proton beam induces RF frequency current between decelerator electrodes and a circuit connected externally, thus the RF frequency potentials are induced on the electrodes, and they travels with almost the same velocity as that of protons in the direction of the beam. The energy of bunched protons is recovered by electric field of this traveling wave. The recovered energy is RF electric energy, and it can be used as the energy source of the modulator and can be supplied to commercial power source.

The numerical and experimental studies were reported previously[2, 8, 4, 5], but the study on energy broadness of the incident flux was not enough. In TWDEC, phase matching between incident particles and traveling wave is so important as it directly affects the conversion efficiency. In the experimental study, the TWDEC simulator used was a small scale, so the thermal energy spread was small. The authors performed a direct energy conversion experiment using the end-loss flux of GAMMA 10 and a CUSPDEC experimental device[6]. According to the examination of the end-loss flux, it has a wide energy spread. The new project of the application of a TWDEC simulator to GAMMA 10 was started[7]. In order to study the dependence on relative energy spread, *bias-type TWDEC* was proposed. All electrodes in the TWDEC is biased with variable negative voltage, and the electrons are repelled by this potential. The incident ions are accelerated, and the relative energy spread can be controlled by the adjustment of the negative bias.

This paper reports the initial result of the experiment applying a TWDEC simulator on GAMMA 10. The next full-scale experiment is in progress with improved electrodes and RF systems. This paper also reports design works of this improvement by showing some results of orbit calculations.

The contents of the paper are as follows. In Sec.2, the initial result of the experiment is presented. The design works for full-scale experiment is presented in Sec.3. The summary of the paper is in Sec.4.

2. Initial results of TWDEC simulator on GAMMA 10

2.1 Experimental arrangement

The TWDEC simulator for GAMMA 10 was installed in the extended tube[6] at the west end of GAMMA 10. The magnetic coils are settled on the tube, and the guiding field can be applied. Fig.1 shows a schematic illustration of the device.

The upper part of the figure indicates inside of the

author's e-mail: takeno@eedept.kobe-u.ac.jp

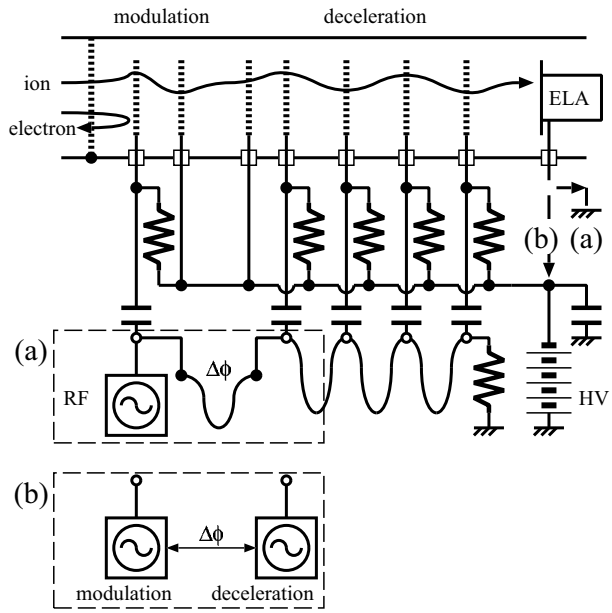

Fig. 1 Schematic illustration of bias-type TWDEC for GAMMA 10.

tube, where grid electrodes are aligned. The first electrode is grounded, and the potential of the remained electrodes can be controlled by not only RF voltage but also DC voltage. The electrodes in the upstream are for the modulator. A pair of uniform modulation fields are formed. In the downstream, the decelerator consisting of over four electrodes is settled. In the real TWDEC, RF voltage on the decelerator electrodes is induced by passing through of density modulated beam. In the simulation experiments, however, the beam current is too small to induce enough voltage for creating deceleration field. Thus, the traveling RF voltage synchronized with the modulator RF is applied to decelerator electrodes by an external RF power source. All grids except the first one can be biased with negative voltage. By applying negative voltage, electrons are expected to be repelled and only ions come into the TWDEC.

In the bottom, an End-Loss Analyzer (ELA) is settled, which has three grids (ion repeller, primary electron repeller, secondary electron repeller) and a collector. Three grids are biased appropriately, and a collector current is measured. In the experiments of this paper, the primary electron repeller and the secondary electron repeller are biased with $-0.8\,\mathrm{kV}$ and $-1.0\,\mathrm{kV}$, respectively, which are enough for repelling electrons in the end-loss flux of GAMMA 10 without an ECH application. The voltage of the ion repeller is varied with shot by shot. In order to evaluate precise effect of the TWDEC, it is necessary to bias the ELA with the same DC voltage[8] as those on the TWDEC electrodes (indicated by '(b)' in the figure). It will be realized in the full-scale experiment and the ELA in the present experiments works on the ground voltage ('(a)' in the figure).

The system needs an RF power source for the modulator and the decelerator. In the initial experiment of the following section, one RF power source is used for both the modulator and the decelerator. The phase difference between the voltage of the modulator and that of the decelerator ($\Delta\phi$) should be controlled. The change of the length of the delay cable is used for this adjustment.

In this RF system (indicated by '(a)' in the figure), the phase difference can be controlled, but the amplitudes of both RF voltage are the same. The new RF system ('(b)' in the figure) is now ready for the next experiment, in which both phase and amplitude for both RF can be controlled independently.

2.2 Experimental results

In the operation of GAMMA 10, the plasma is produced and heated by an application of ICRF with gas puffing following to the injection of seed plasma by plasma guns. The perpendicular ion temperature of the central cell is 3-5 keV, and the parallel one is estimated to be 0.2-0.4 keV. During the ICRF pulse, ECH is applied for higher confinement of the plasma, when the electrons are heated and high energy electrons are created. The objective plasma in this paper, however, is the one without ECH, so the electron temperature of the central cell is about 0.1 keV, and high energy electrons do not exist. In this condition, the plasma potential at the central cell is 0.3-0.5 kV, and those at the plug cells are the same or slightly lower.

In the initial experiment, DC bias voltage was not applied, and only RF voltage was used. The ELA signal of collector current I_C was measured with other signals of GAMMA 10 plasma. The effect of guiding field was confirmed that the collector current increased as the intensity of guiding magnetic field was enhanced.

The reaction of collector current due to RF application was observed. A typical example of time evolutions of signals is shown in Fig.2, where (a) diamagnetic signal, (b) line density, and (c) collector current of DEC ELA. RF voltage was applied during 20 ms pulse as in the figure as shown at the top of the figure, when there was no ECH application. According to the figure, the collector current increases during RF pulse. The increment of the collector current was changed by the voltage of ion repeller of ELA (V_{IR}) and RF conditions.

In order to evaluate the increment of I_C, the time averaged value of I_C was calculated for $110 \sim 130\,\mathrm{ms}$ and $135 \sim 145\,\mathrm{ms}$ in the same shot: the former value is I_C for RF on, and the latter one is for RF off. The difference between them is the increment of collector

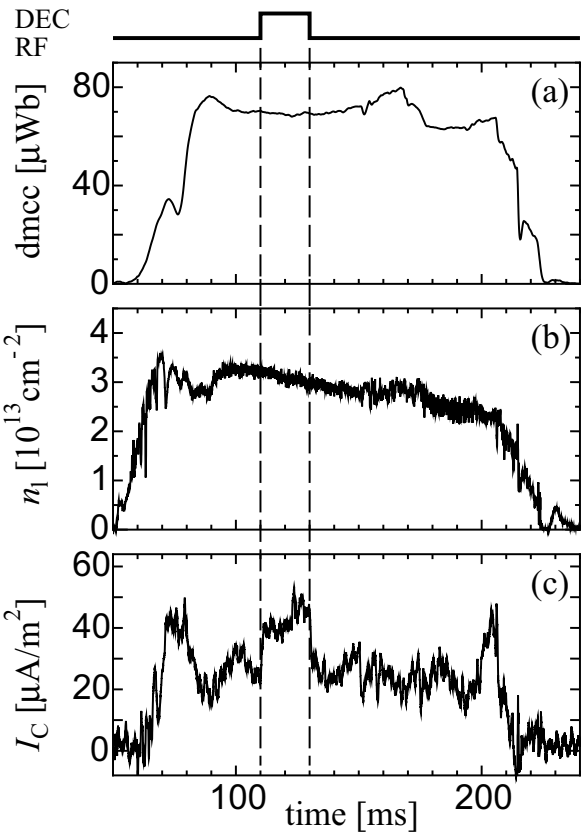

Fig. 2 A typical example of time evolutions of (a) diamagnetic signal, (b) line density, and (c) DEC ELA signal (collector current).

current ($\Delta I_{\rm C}$).

The data are summarized as Fig.3 where $\Delta I_{\rm C}$ is shown as a function of $V_{\rm IR}$. This roughly means the variation of the amount of ions for each energy corresponding to $V_{\rm IR}$. From Fig.3, it is found that dependence of $\Delta I_{\rm C}$ on $V_{\rm IR}$ varies according to the phase difference $\Delta\phi$. For $\Delta\phi = 90$ degree, increment of low energy ($V_{\rm IR} \leq 0.2$kV) is large and that of high energy ($V_{\rm IR} \geq 0.4$kV) is small. On the contrary, for $\Delta\phi = 180$ degree, increment of high energy ($V_{\rm IR} = 0.8$kV) is relatively large though increment of low energy ($V_{\rm IR} \leq 0.4$kV) is not so large.

This is natural because a TWDEC uses the principle of inverse process of a linear accelerator, so it works as not only a decelerator but also an accelerator owing to $\Delta\phi$[9]. When the bunched particles in the modulated beam arrive at the entrance of the decelerator, an appropriate $\Delta\phi$ provides deceleration field for those particles. In such a case, particles are always in the deceleration field as the field is running in the same velocity with the particles, resulted the device works as a decelerator. On the contrary, another appropriate $\Delta\phi$ provides acceleration field for the bunched particles, and they are always in the acceleration field resulted the device works as an accelerator. In the

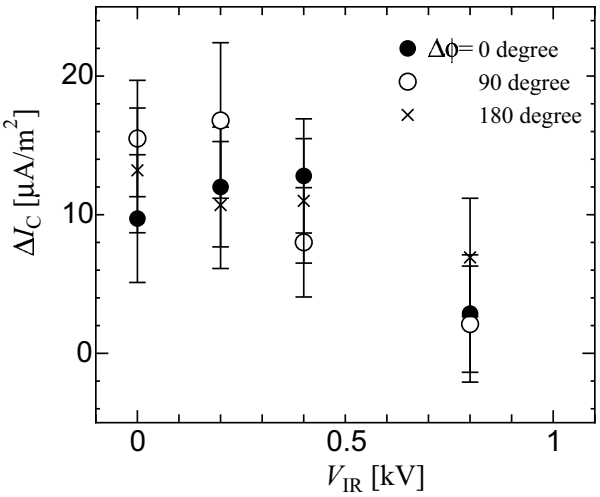

Fig. 3 Increment of collector current due to application of RF versus voltage of the ion repeller.

precise discussion, the device is designed as a decelerator, so the accelerated particles are not always in the acceleration field because phase matching is lost after a large acceleration. However, the decelerator in the present experiment is short, so phase matching is not lost during passing through the decelerator. As a result, contrasted results due to $\Delta\phi$ are possible to be obtained in the present experiment.

2.3 Comparison with orbit calculation

This variation due to $\Delta\phi$ is confirmed by 1-D orbit calculations[5]. The calculation code was extended that the incident proton flux had a shifted Maxwellian distribution:

$$f(E) \propto (E - E_{\rm s})^{0.5} \exp\left(-\frac{E - E_{\rm s}}{T}\right) \qquad (1)$$

where T is parallel proton temperature and $E_{\rm s}$ is constant. In the calculation, $E_{\rm s} = 300\,$eV and $T = 300\,$eV, and the same positions of electrodes as the experiment are settled. The amplitude of the RF is $100\,{\rm V}_{0p}$, which is also the same as the experiment. The energy distribution of the protons passing through the TWDEC is examined and shown in Fig.4(a). The abscissa is the energy of protons (E), and the ordinate is the number of protons in which a moving average is applied to eliminate noisy components caused by finite number of particles. According to the figure, the difference among three cases for $\Delta\phi$ is rather small.

In order to compare the experimental results, $V_{\rm IR}$-$I_{\rm C}$ characteristic is simulated by using

$$I_{\rm C}(V_{\rm IR}) \propto \int_{eV_{\rm IR}}^{\infty} N(E)\sqrt{E}dE \qquad (2)$$

where e is a unit charge and $N(E)$ is the number of protons with an energy of E. The obtained $I_{\rm C}$

for each $\Delta\phi$ ($I_{C-\alpha}$ denotes I_C for $\Delta\phi = \alpha$ degree in the following) is normalized by the averaged value ($(I_{C-0} + I_{C-90} + I_{C-180})/3$), and shown in Fig.4(b). The same symbols as Fig.3 are attached to distinguish the curves for $\Delta\phi$. From this figure, the same tendency with Fig.3 can be seen For $\Delta\phi = 90$ degree, I_C is relatively large in the low energy, but it is relatively small in the high energy. On the contrary, for $\Delta\phi = 180$ degree, vice versa.

Although the evaluation is rather rough, the ion flux flowing into the TWDEC simulator was affected by RF field, and the reaction is not inconsistent with the TWDEC operation. The continuous variation of I_C to V_{IR} is necessary to obtain a variation of distribution functions and conversion efficiency which will be performed in the next full-scale experiment.

3. Design work of improvement of electrode and RF system

3.1 Characteristics of modulator for wide energy spread flux

In the TWDEC employing a modulator of single uniform RF field, the problem of modulator design is a trade-off between a conversion efficiency and a length of the device. The high modulation voltage (V_m) results in the wide energy spread of the beam, and thus the low conversion efficiency. On one hand, the theoretical expression of the bunching length includes a factor of V_m in the denominator, that means low modulation voltage results in long length of the device. Small scale simulators have a limitation of the device length. Moreover, another problem is also caused that beam transfer for long length results in the divergence of the beam.

The TWDEC simulator for GAMMA 10 also has significant limitation of the length of the device. The previous modulation system (Fig.1(a)) was designed with considering this limitation. By employing a pair of uniform RF field appropriately, the bunching length can be shortened. In the new design, the wide energy spread was also taken into account.

The 1-D orbit calculation code with a shifted Maxwellian distribution incident flux was employed again. According to a typical experimental result, $E_s = 100$ eV and $T = 400$ eV were taken, and just one modulator consists of a pair of uniform field was settled at $0 \sim 0.06$ m. The axial distribution of protons in the steady state was examined.

The calculation results are shown in Fig.5. Fig.5(a) indicates samples of axial distribution for $t = 0, T_{RF}/4, T_{RF}/2, 3T_{RF}/4$, where T_{RF} is a period of applied RF, for $V_{mod} = 250\,V_{0p}$. The peak in the graphs means a bunching of protons, and it is found that they moves to the right hand. When those graphs are mapped to the deepest plane, the envelope

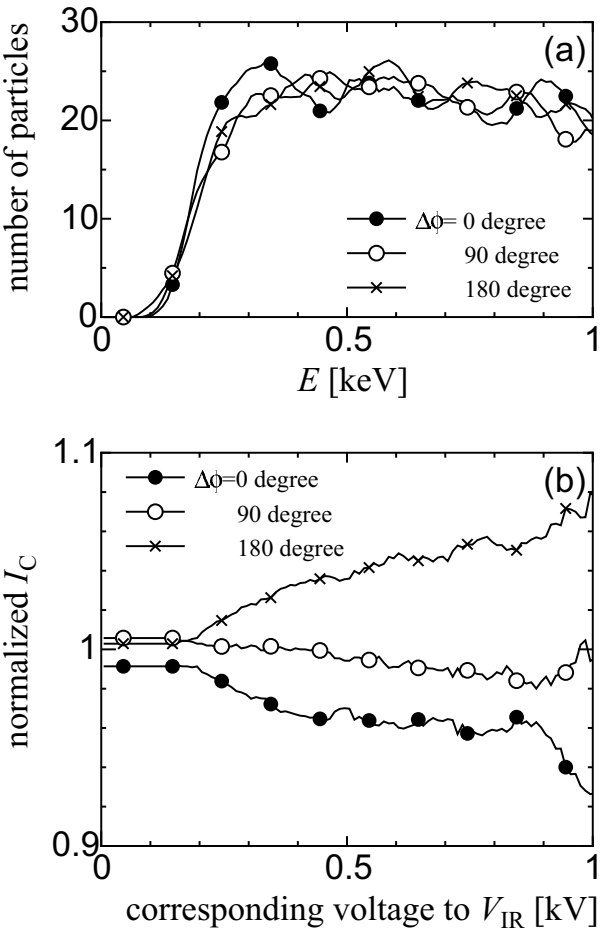

Fig. 4 Results of orbit calculations. Here, (a) calculated energy distribution of protons passing through the TWDEC in the same condition with experiments, and (b) simulated V_{IR}-I_C characteristic with taking a normalized value in the ordinate.

as shown in the figure by thick curve is obtained (noisy components caused by finite number of particles are eliminated by a moving average). This envelope indicates amplitudes of density oscillation, and the peak of the envelope means a bunching point where the entrance of the decelerator should be settled.

In the same way, envelopes for $V_{mod} = 300$ and $400\,V_{0p}$ are also calculated and shown in Fig.5(b). According to the figure, the extent of the bunching becomes well as the modulation voltage increases. As for the bunching point, it is found to be almost the constant of 0.13 m even if the modulation voltage is varied. This is quite different from the case of narrow spread flux, and is the effect of the energy spread. The usual characteristic was found that the bunching length became short as the modulation voltage increased when we set the lower T. This results means that V_{mod} should be adjusted appropriately. The modulation voltage is independently controlled in the new system (Fig.1(b)).

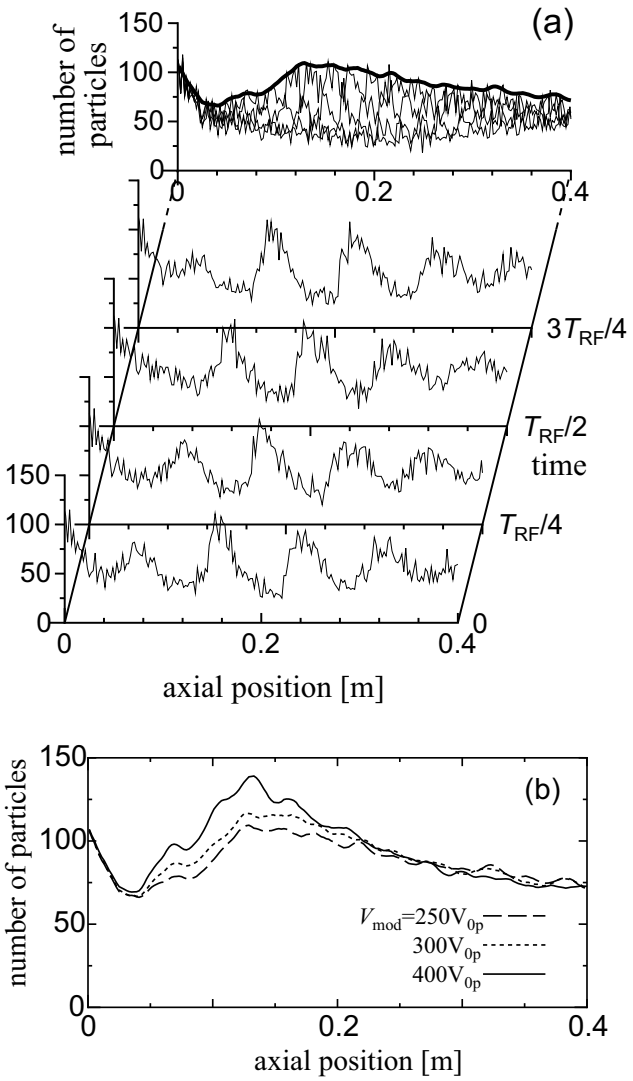

Fig. 5 Particle distribution along the axis. Here, (a) indicates how to obtain an envelope, and (b) shows envelopes for some modulation conditions.

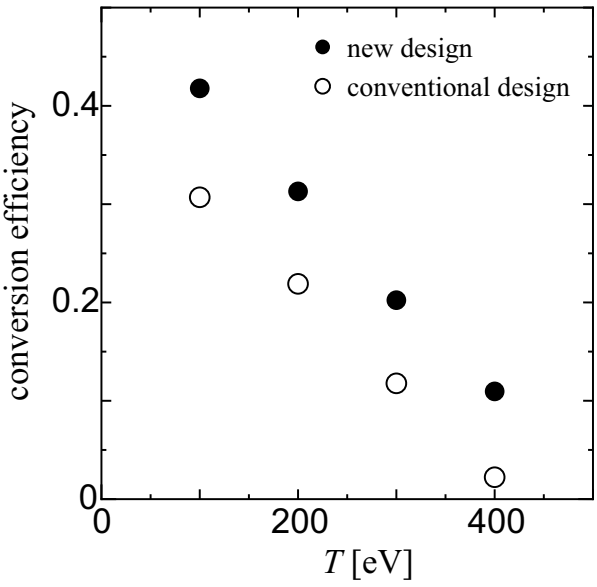

Fig. 6 Conversion efficiency as a function of incident parallel proton temperature. Open circles are for a decelerator designed by conventional method, and closed circles are for that by new method.

3.2 Employment of new design method for decelerator electrodes

In the previous experiments, the decelerator was designed as shown in Ref.[5]. In this method, the particles with an average incident velocity was taken as an object, and the optimum deceleration field for this object particle is constructed.

There is another design method shown in Ref.[8]. The particle distribution in the phase space is considered in this method. An appropriate traveling wave field is constructed, and the particles with an averaged incident velocity will be decelerated with a constant deceleration. Large part of the particles are trapped in the valley of potential of traveling wave and decelerated with a bounce motion in the valley. In the case of the flux with wide energy spread, a lot of particles will appear which has less velocity matching with a traveling wave when we design by the former conventional method. For the flux with wide energy spread, the latter new method will have larger capability to trap particles with less velocity matching. Moreover, the variation of the deceleration along the axis is too large in the conventional method, so the number of electrodes are limited to construct with enough accuracy.

We confirm this consideration by using 1-D orbit calculation. Fig.6 shows conversion efficiency as a function of incident proton temperature. The modulator used in this calculation is that in Fig.5(a) and the DC bias of $-1.5\,\mathrm{kV}$ is supplied. The structure of the decelerator was designed for $T = 400\,\mathrm{eV}$, and the same structure is used for other values of T, but the value of E_s was adjusted to keep the averaged energy of the particle matches with the designed value. Open circles are for the conventional method, in which the number of electrodes are limited to be six, and closed circles are for the new method which has eight electrodes. According to the figure, the new method provides better efficiency than the conventional method. The efficiency decreases as T increases, but about 10% is kept fro $T = 400\,\mathrm{eV}$ in the case of new design although it is nearly zero in the case of conventional one. The new method is desirable and it is employed in the new electrodes system.

4. Summary

In order to examine the operation characteristics of TWDEC for the incident particle flux with a wide energy spread, a bias-type TWDEC simulator was installed at the end of GAMMA 10. The initial exper-

imental was performed and the result obtained was not inconsistent with an expected TWDEC characteristics. For the next full-scale experiment, the design of modulator and decelerator was examined. The bunching position is not so changed for a flux with a wide energy spread, so the independent amplitude adjustment of modulation voltage is desirable. The deceleration electrodes should be designed by a new method which provides trapping of large part of the particles in the potential valley of traveling wave. The full-scale experiments with the new system is in progress and will be reported in the near future.

Acknowledgment

The authors acknowledge valuable discussions with Drs. Y. Tomita, M. Ishikawa. This work was supported in part by the bilateral coordinated research between Plasma Research Center, Univ. Tsukuba, National Institute for Fusion Science, and Kobe University.

[1] H. Momota, LA-11808-C, Los Alamos Natl. Lab., 8 (1990).
[2] K. Sato, et al., Proc. 7th Int. Conf. Emerging Nuclear Energy Systems, 1993 517 (1994).
[3] H. Shoyama, et al., J. of Plasma and Fusion Res. **72** 439 (1996).
[4] K. Noda and Y. Yasaka, Fusion Technol. **33**, 93 (1998).
[5] H. Takeno, et al., Jpn. J. of Appl. Phys. **39**, 5287 (2000).
[6] Y. Yasaka, et al., Trans. Fusion Sci. Technol. **51**, 171 (2007).
[7] D. Omoya, et al., Trans. Fusion Sci. Technol. **55**, 114 (2009).
[8] Y. Nakashima, et al., Appl. Phys. Letters **54**, 2642 (1989).
[9] M. Ishikawa, et al., Fusion Engineering and Design **81**, 1689 (2006).